Electronic properties of GaSe, InSe, GaS and GaTe layered semiconductors: charge neutrality level and interface barrier heights

2015 Semicond. Sci. Technol. 30 115019

(http://iopscience.iop.org/0268-1242/30/11/115019)

IOP Publishing Semiconductor Science and Technology
Semicond. Sci. Technol. 30 (2015) 115019 (9pp) doi:10.1088/0268-1242/30/11/115019

Electronic properties of GaSe, InSe, GaS and GaTe layered semiconductors: charge neutrality level and interface barrier heights

V N Brudnyi[1], S Yu Sarkisov[2,4] and A V Kosobutsky[1,3]

[1] Nanolectronics and Nanophotonics Laboratory, Tomsk State University, Tomsk 634050, Russia
[2] Functional Electronics Laboratory, Tomsk State University, Tomsk 634050, Russia
[3] Department of Physics, Kemerovo State University, Kemerovo 650043, Russia

E-mail: brudnyi@mail.tsu.ru, sarkisov@mail.tsu.ru and kosobutsky@kemsu.ru

Received 1 August 2015, revised 24 September 2015
Accepted for publication 24 September 2015
Published 16 October 2015

Abstract

Density functional theory calculations have been applied to study the structural and electronic properties of layered ε-GaSe, γ-InSe, β-GaS and GaTe compounds. The optimized lattice parameters have been obtained using vdW-DF2-C09 exchange-correlation functional, which is able to describe dispersion forces and produces interlayer distances in close agreement with experiments. Based on the calculated electronic band structures, the energy position of the charge neutrality level (CNL) in the III–VI semiconductors has been estimated for the first time. The room-temperature values of CNL are found to be 0.80 eV, 1.02 eV, 0.72 eV and 0.77 eV for ε-GaSe, β-GaS, GaTe and γ-InSe, respectively. The persistent p-type conductivity of the intentionally undoped ε-GaSe, β-GaS and GaTe and n-type conductivity of γ-InSe crystals are discussed and explained using the concept of CNL. We also estimated the barrier heights for a number of metal/semiconductor and semiconductor/semiconductor interfaces assuming partial Fermi level pinning at the CNL. A reasonable agreement between our calculations and the available experimental data has been obtained.

Keywords: charge neutrality level, III–VI semiconductors, interface barrier, van der Waals density functional calculation

(Some figures may appear in colour only in the online journal)

1. Introduction

III–VI compounds GaSe, GaS, GaTe and InSe are layered crystals with strong ionic-covalent bonds within the layers and predominantly van der Waals bonding (about 2 orders of magnitude weaker) between them [1]. For the majority of III–VI semiconductors a number of polytypes were identified, which differ by the stacking of the adjacent layers. Due to their lamellar structure all III–VI polytypes exhibit highly anisotropic optical, mechanical and electronic properties. Besides a high level of anisotropy, the III–VI crystals have several interesting peculiarities which have been discussed in the literature. First, the intentionally undoped typical GaSe, GaS, GaTe and InSe samples possess a persistent type of conductivity which is difficult to change by standard methods of chemical doping. Second, the bonds on the van der Waals surface (0001) are saturated [2] and therefore the absence of dangling bonds and surface states has been assumed. As a result, the (0001) surface in III–VI semiconductors is not reactive and is considered as atomically abrupt [3]. Numerous studies by LEED, Auger and photoemission spectroscopy confirm the high quality of III–VI semiconductors (0001) surface (for example [3] and references therein). Therefore, the absence of Fermi level pinning at the free (0001) surface can be asserted. Finally, strong lattice mismatch in the heterostructures composed of the lamellar III–VI and three-dimensional semiconductors is accommodated within few atomic planes through the relaxation process in III–VI layers

[4] Author to whom any correspondence should be addressed.

and therefore no strain effects occur at the interfaces. So, the III–VI films are considered promising for use as interlayer buffers between the highly mismatched semiconductors in the heteroepitaxial systems with Si, III–V and II–VI group compounds, Al_2O_3 [4, 5] etc.

The band structure energies and the lattice parameters of III–VI semiconductors have been theoretically investigated using density functional theory (DFT) with standard LDA and GGA exchange-correlation functionals [6–8]. Recently a number of DFT-based dispersion techniques have been developed that extend the density functional approach to long-range forces [9–11]. An adequate description of the van der Waals forces is a crucial factor in the first-principles calculations of the parameters intrinsically determined by interlayer interactions in III–VI compounds, like interlayer distances or binding energies. In our work we have computed first the optimized lattice constants of ε-GaSe, γ-InSe, β-GaS and GaTe employing advanced density functional with a non-local correlation term [9]. In a next step, these optimized lattice parameters were used to calculate the band structure energies, which, in turn, were employed as input data in the charge neutrality level (CNL) calculations.

CNL is one of the semiconductor vital parameters which defines electronic properties of the defective material (both in bulk and on the surfaces), the energy diagrams of the metal/semiconductor (M/S) and semiconductor/semiconductor (S/S) interfaces. The location of CNL in the semiconductor band structure corresponds to the energy where the gap states change from the predominantly valence-band-like to the conduction-band-like. With the only exception of GaSe [12, 13], the CNLs have not yet been calculated for III–VI compounds. In the last part of the paper we perform an analysis of the influence of CNL position on the electronic properties of III–VI materials and on the energy diagrams of a number of M/S and S/S interfaces with III–VI semiconductors. One of the paper's goals was to test how the obtained CNL values allow to explain the present experimental data on the persistent type of conductivity observed in GaSe, GaS, GaTe and InSe and to estimate the M/S barrier heights and the S/S interface band offsets for a number of heterostructures based on III–VI compounds.

2. Electronic band structures

2.1. Computational details

Electronic structure calculations have been performed within DFT using projector augmented wave (PAW) method, as implemented in the Quantum ESPRESSO [14] package. The outer s- and p-electrons of Ga, In, S, Se and Te atoms were included in the valence shell. Besides these, the 3d states of Ga and 4d states of In and Te atoms were also treated as valence. To ensure high accuracy of DFT calculations, the plane wave cutoff energy was set to 50 Ry, and the Brillouin zones (BZs) of the crystals under study were sampled with sufficiently dense *k*-point meshes. The total energies were considered converged when the energy difference between two consecutive self-consistent iterations was less than 0.001 mRy. The previous theoretical works showed that the spin–orbit effects play only a minor role in the III–VI compounds [6]. Therefore, we did not include spin–orbit interaction in the present calculations.

The band structure calculations have been performed for the optimized crystal structures. The structure optimization was carried out using a standard BFGS algorithm, and the equilibrium geometries were obtained when the Hellmann–Feynman forces acting on all atoms were smaller than 2 meV $Å^{-1}$. Due to a predominant role of the van der Waals interaction in the interlayer bonding, a choice of the exchange-correlation functional is essential for correct description of the structural properties of layered materials. As it was demonstrated in [13], the recently developed van der Waals density functional vdW-DF2 [9] combined with a Cooper exchange flavor $C09_x$ [10] as well as the semi-empirical DFT-D2 [11] method offer very good performance in case of GaSe compound. By construction, vdW-DF2-C09 includes the specially designed exchange and non-local correlation terms (with the second version of the vdW kernel [9]) being dependent only on the electron density. This approach is entirely in the spirit of DFT as opposed to the DFT-D2 scheme. In this work, the PBE-GGA [15] and vdW-DF2-C09 functionals were employed at the stage of structure optimization and their results have been compared and analyzed.

2.2. Lattice parameters and band structures

The layered III–VI compounds are known to crystallize in a number of polymorphic modifications, the most common of which are ε-, β-, γ- and δ-polytypes [1]. The corresponding space groups are $P\bar{6}m2$, $P6_3/mmc$, R3m and $P6_3mc$. The ε-, β- and δ-polytypes have hexagonal crystal lattice with 8 or 16 atoms in the unit cell [16, 17], while γ-polytype has a rhombohedral lattice (4 atoms in the cell) [18]. Bridgman-grown single crystals of GaSe are usually of ε-polytype with a small admixture of γ-GaSe whereas the most stable forms of GaS and InSe are β and γ correspondingly. The diversity of crystal modifications of III–VI compounds is due to a possibility of different stacking of the layers with respect to each other. All the layers of GaS, GaSe and InSe have the same structure and hexagonal symmetry to be built up of four parallel atomic sublayers stacked in the order VI–III–III–VI, i.e. two atomic planes filled by metal atoms from III group of the Periodic system are sandwiched between two planes of S, Se or Te atoms.

Gallium telluride (GaTe) occupies a special place among the III–VI compounds, since its layers have some peculiarities in the atomic arrangement compared to GaS, GaSe and InSe. While in the latter all cation–cation bonds are oriented perpendicular to the layers, in GaTe one-third of the Ga–Ga bonds lie almost parallel to the layer planes. As a result, the GaTe crystal is monoclinic with space group $B2/m$ (12 atoms in the unit cell) [19]. It should be pointed out that, in consequence of its more complicated structure, GaTe does not exhibit any polytypism unlike other III–VI semiconductors.

Table 1. Calculated using PBE and vdW-DF2-C09 functionals and experimental [16–19] lattice parameters a, b, c, γ, layer thickness d_{intra} and interlayer distance d_{inter} in a series of III–VI compounds. The lengths are given in angstroms and angles (γ) in degrees. The percentage differences (Δ) between the calculated and experimental values are also shown.

		PBE	Δ	vdW-DF2-C09	Δ	Expt.
β-GaS	a	3.633	1.3	3.575	−0.3	3.587
	c	16.677	7.6	15.460	−0.2	15.492
	d_{intra}	4.638	0.8	4.613	0.3	4.599
	d_{inter}	3.701	17.6	3.117	−1.0	3.148
ε-GaSe	a	3.823	2.1	3.761	0.5	3.743
	c	17.848	12.1	15.943	0.2	15.919
	d_{intra}	4.819	0.9	4.783	0.2	4.776
	d_{inter}	4.106	29.0	3.189	0.2	3.184
γ-InSe	a	4.091	2.2	4.028	0.6	4.002
	c	26.982	8.2	24.996	0.2	24.946
	d_{intra}	5.368	1.6	5.355	1.4	5.281
	d_{inter}	3.626	19.4	2.977	−1.9	3.035
GaTe	a	17.896	2.8	17.373	−0.2	17.404
	b	10.688	2.2	10.461	∼0.0	10.456
	c	4.144	1.6	4.089	0.3	4.077
	γ	105.32	0.8	104.24	−0.2	104.44
	d_{intra}	5.438	1.0	5.400	0.3	5.384
	d_{inter}	2.255	8.9	2.039	−1.5	2.071

The computed lattice parameters and interatomic distances of the III–VI crystals under study are listed in table 1. Note that for γ-InSe the hexagonal parameters are provided for simplicity of comparison. For the analysis of the theoretical data, the percentage differences between the calculated and experimental values are given after each column with the theoretical results.

In case of materials with ionic or covalent bonding, the structural investigations in the framework of DFT with typical LDA or GGA exchange-correlation functionals (with PBE-GGA being a 'standard' one) usually produce sufficiently accurate results [20, 21]. In previous theoretical works on III–VI semiconductors the PBE functional was also typically used [6–8]. However, the class of layered compounds with a considerable admixture of the van der Waals forces in the interlayer bonding needs a more advanced computational approach. Here we compared the results of structural optimization using PBE and vdW-DF2-C09 functionals. The vdW-DF2 adds a non-local correlation energy to the semi-local exchange functional PW86 [9] to describe properly both short-range covalent bonds and long-range van der Waals forces. The vdW-DF2-C09 functional is a variant of vdW-DF2, which replaces PW86 with the exchange functional $C09_x$ of Cooper [10].

As one can see, PBE-GGA significantly overestimates the experimental lattice parameter c of GaS, GaSe and InSe by 7.6%–12.1%. The maximum overestimation, 12.1%, is found in case of GaSe. Note that in our previous work on GaSe the similar effect was found [13], but the difference between the calculated and measured c values did not exceed 7.7%. We attribute the increased difference to the more accurate PAW method employed in the present calculations while norm-conserving pseudopotentials were used in [13].

The overestimation of the lattice parameter c is due to strong overestimation of the interlayer distance d_{inter}, the 'van der Waals gap', by 9%–29% (table 1). On the other hand, the bonds within the layers have a strong covalent character and PBE expectedly gives lattice constant a and layer thickness d_{intra} in reasonable agreement with measured values. Note that in case of monoclinic GaTe the anion atoms lie at the different distances from the middle of the layer. Therefore, for this compound we define d_{intra} as the distance between the planes of outer Te atoms. In [13] we found that vdW-DF2 functional is too repulsive in description of GaSe lattice properties. The present PAW calculations show that in comparison with PBE and vdW-DF2, the vdW-DF2-C09 systematically improves all interatomic distances, both interlayer and intralayer. Indeed, in this case the difference between theoretical and experimental values of c does not exceed 0.3%. As is seen from table 1, this remarkable improvement is achieved due to accurate reproduction of the interlayer spacing.

The theoretical lattice constants and atomic positions obtained with vdW-DF2-C09 functional were used as input data for subsequent electronic band structure calculations. The results of these calculations are presented in figure 1.

We do not show the lower occupied bands formed by anion s states as well as almost flat bands originated from the semicore Ga 3d and Te 4d states, which are located at about 14.9 eV and 36.7 eV below the top of the valence band, respectively. Due to different number of formula units in the primitive unit cell, the band structures of the studied compounds include different number of the valence bands in the range from −8 to 0 eV, namely, 14 bands for GaS and GaSe, 7 for InSe and 21 in case of GaTe. As can be seen, the band structures of β-GaS and ε-GaSe with hexagonal crystal lattice are very similar to each other. However, there are some differences to be mentioned: (i) when going from β- to ε-polytype, the point symmetry of the crystal lattice decreases and this removes degeneracy of the energy levels at k-points on the A–H line, and (ii) the valence bands of GaS have a slightly larger dispersion in the k-space. The latter can be attributed to the smaller length of the cation–anion interatomic distances in GaS which leads to a stronger orbital hybridization.

The results of our electronic structure calculations for InSe and GaTe are in close agreement with the recent pseudopotential and full-potential calculations [6, 8]. Because of the different BZs, the energy dispersion of the valence and conduction bands of InSe and GaTe can not be directly compared with those of GaS and GaSe. Nevertheless, it should be noted that a character of atomic orbitals hybridization has many common features. The valence bands in the range from −8 to −4 eV are composed mainly of Ga 4s or In 5s states with significant contribution of anion p states. The uppermost energy levels in the range from about −4 to 0 eV (valence band top) are formed predominantly by anion and cation p states with a small admixture of s orbitals of the

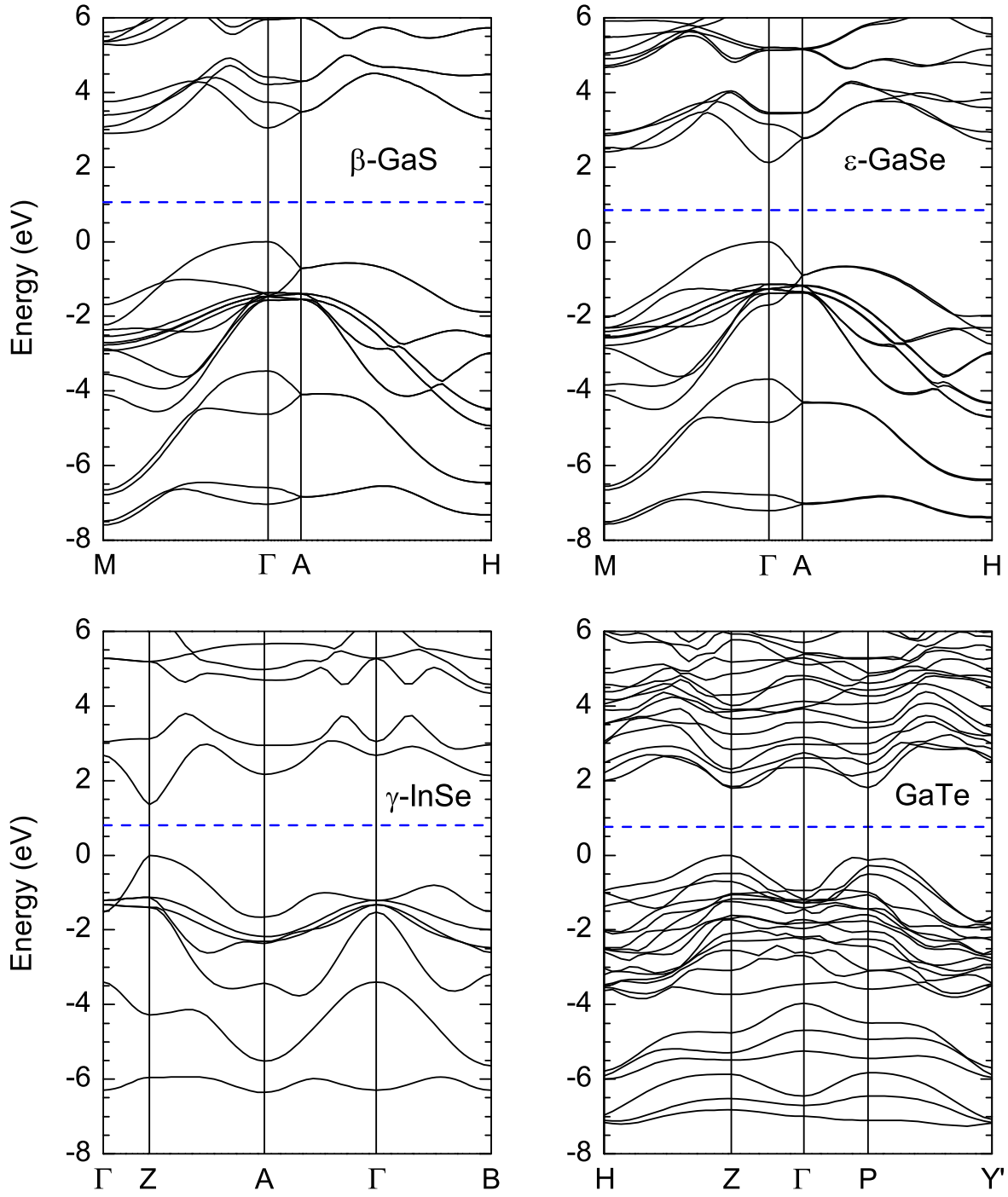

Figure 1. Band structures of β-GaS, ε-GaSe, γ-InSe and GaTe compounds. The dashed lines indicate the location of CNL at low temperature (see table 2). The valence band maximum is set at zero energy.

metal. An analysis of partial contributions from S and Se atoms to the total electronic density of states also elucidates the significant role of p_z orbitals of the anion, which contribute to the states near the valence band top of GaS, GaSe and InSe and thereby determine the particular features of the upper valence band.

In agreement with previous results, our calculations show that the maximum of the valence band is at the Γ point for GaS and GaSe and at the *Z* point in case of InSe and GaTe. However, the theoretical band gap energies (E_g) are underestimated due to the well-known limitations of DFT calculations within LDA or GGA. The experimental low-temperature ($T = 1.6$–77 K) values of E_g are 2.60 eV (β-GaS), 2.12 eV (ε-GaSe), 1.35 eV (γ-InSe) and 1.80 eV (GaTe) from measurements [22–24]. The corresponding room temperature (RT) values are 2.53 (β-GaS), 2.01 eV (ε-GaSe), 1.26 eV (γ-InSe) and 1.69 eV (GaTe) [22–25]. Our calculations of the CNL were based on the experimental E_g values to improve the accuracy of prediction both the CNL and related quantities.

Table 2. CNL_{1-3} positions with respect to the valence band top, their averaged value CNL and experimental E_g gaps at the RT/LT conditions, and also Φ_v, $CNL^{abs} = (\Phi_v—CNL)$ and WF at RT for ε-GaSe, γ-InSe, β-GaS, GaTe and Si. All values are in eV. The values obtained by extrapolation are marked by asterisk.

Material	CNL_1	CNL_2	CNL_3	CNL	E_g	Φ_v	CNL^{abs}	WF
ε-GaSe	0.80/0.86	0.74/0.79	0.86/0.91	0.80/0.85	2.01/2.12(Γ_c–Γ_v)	5.72	4.92	5.00
γ-InSe	0.77/0.82	0.73/0.77	0.81/0.85	0.77/0.81	1.26/1.35(Z_c–Z_v)	5.80	5.03	4.91*
β-GaS	1.07/1.11	0.93/0.96	1.07/1.10	1.02/1.06	2.53/2.60(M_c–Γ_v)	6.50	5.48	5.44*
GaTe	0.74/0.79	0.67/0.71	0.75/0.80	0.72/0.77	1.69/1.80 (Z_c–Z_v)	4.95	4.23	4.62*
Si	0.34/0.37	0.36/0.39	0.44/0.47	0.37/0.41	1.12/1.20 (X_c–Γ_v)	5.10	4.73	4.83

3. Charge neutrality level

The concept of CNL is widely used in the physics of semiconductors [26]. The CNL location in the energy spectrum of a semiconductor determines electronic properties of the defect-containing material, the energy band diagram at M/S and S/S interfaces and the surface Fermi level position. In the present work we used the following three analytical models to estimate the CNL position in ε-GaSe, γ-InSe, β-GaS and GaTe compounds.

In the 'mid-gap level' model the CNL position is identified with the middle of the isotropic energy gap $<E_g>$ averaged over the entire BZ of the crystal, which is close to the dielectric (Penn's) gap [26]

$$CNL_1 = <E_g>/2. \quad (1)$$

In the 'amphoteric level' model the CNL is obtained from the neutrality condition at the local gap center which is fulfilled at $E = CNL$ due to compensation of positive and negative charges connected with the valence and conduction bands of the semiconductor, respectively [26, 27]

$$\partial G_0\left(E, CNL_2\right)/\partial E = 0. \quad (2)$$

In the deep-level model the CNL value is determined as the deepest (most localized) gap state within the energy region including the forbidden gap of the crystal [27]

$$\partial^2 G_0\left(E, CNL_3\right)/\partial E^2 = 0. \quad (3)$$

Here G_0 is the Green's function of the crystal averaged over the unit cell.

It should be noted that convergence of the CNL calculations depends mainly on the number of electronic energy bands included in such computations and to a lesser degree on the BZ sampling. In order to obtain sufficiently accurate results, we have calculated 200 bands (i.e., 38 occupied and 162 conduction bands) on a regular $12 \times 12 \times 2$ mesh of k-points for β-GaS and ε-GaSe, 100 bands on a $8 \times 8 \times 8$ k-mesh for γ-InSe and 300 bands on a $8 \times 8 \times 4$ k-mesh in case of GaTe crystals. These energies were used as input data in expressions (1)–(3). A series of convergence tests demonstrated that the CNL positions in most cases converge to within 0.01 eV. Before final calculations of the CNL the underestimated theoretical band gaps were adjusted by a rigid upward shift of the conduction bands to match the above-mentioned experimental data.

The computed CNL positions according to expressions (1)–(3) at RT and at $T = 0$–77 K (LT) as well as the related band gaps, the valence band top position with respect to vacuum level (Φ_v) and the photoelectron work function (WF) are presented for III–VI and Si semiconductors in table 2.

The data for silicon are included for a confirmation of our numerical calculation results as Si is the most studied semiconductor. The CNL values for Si at 0 K are taken from [27], while at RT the corresponding values have been derived using the coefficient $\partial CNL/\partial T \approx -1.10^{-4}$ eV K^{-1} [26]. The E_g values at RT/LT are adopted from the measurements: ε-GaSe [22], γ-InSe [23], GaTe [24], β-GaS [22, 25]. The values of Φ_v are borrowed from: ε-GaSe and γ-InSe [28], GaTe [29], β-GaS [30], Si [31]. The experimental WF value of undoped GaSe is equal to 4.6 ± 0.2 eV [32], while in p-doped GaSe with Fermi level position near $E_V + (0.1$–$0.2)$ eV the WF = 5.4 eV [33]. The averaged value is given in table 2. For Si the experimental WF value is equal to 4.83 eV [31]. To estimate WF of γ-InSe, β-GaS and GaTe we used the expression $WF^* = (WF_c \cdot WF_a)^{1/2}$, where WF_c (WF_a) are the cation (anion) photoelectron WFs taken from [34]. In the case of sulfur we adopted WF(S) = 6.5 eV because $WF_a \approx \Phi_v$ in the semiconductors. As shown in table 2 the CNL^{abs} is equivalent to the WF(WF^*) value, i.e. both of these values represent the semiconductor surface Fermi level position.

4. Type of conductivity

It is known that CNL determines electronic properties of the defective semiconductors, for example ones irradiated with high energy electrons, neutrons or ions. Moreover such defective materials are used to determine CNL value from the Hall or thermo-EMF measurements [26, 27]. The semiconductors which contain a lot of grown-in defects demonstrate the stable type of electrical conductivity and CNL position in their energy spectra may be the key to understand this phenomenon.

The intentionally undoped III–VI semiconductors display a persistent type of conductivity that restricts their applications. For example, GaSe crystals grown by Czochralski or Bridgman methods show p-type conductivity with electrical resistivity of 10^3–10^9 Ω cm at RT [1]. The same behavior is observed in GaS ingots pulled from the melt or prepared by

the sublimation method [35] and also in the as-grown GaTe crystals [36]. Thus, the undoped GaSe, GaS and GaTe semiconductors have p-type conductivity, while at the same time the as-grown samples of InSe compound are always of n-type with an electron concentration of the order of 10^{15} cm^{-3} [37]. The observed types of conductivity correlate with the calculated CNL energy position in the forbidden gap of these materials. This phenomenon is well known for some other semiconductors. For example, the intentionally undoped InN has a stable n^+-type conductivity due to CNL location within the conduction band continuum, while a p^+-type of as-grown GaSb is determined by the CNL position near the valence band top. It is supposed that electronic properties of these materials are affected by the grown-in defects. As follows from our calculations, CNL is located in the upper half of InSe forbidden gap and deeply in the lower half of GaSe, GaS and GaTe forbidden gaps. Such CNL energy position in III–VI semiconductors is energetically favorable for the donor-type defect formation in the InSe crystals and for the deep acceptor-type defect formation in GaSe, GaS and GaTe compounds during the growth process.

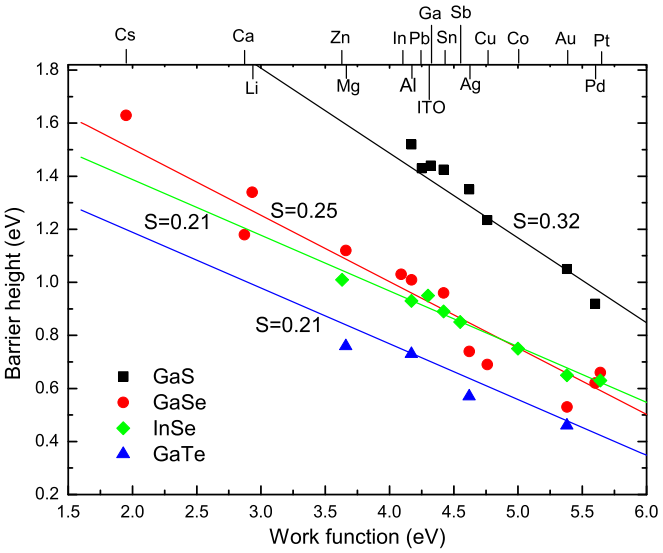

Figure 2. M/S barrier heights for the holes $\Phi_{bS}{}^{p}$ versus the contact metal work function Φ_m for ε-GaSe [41, 42], γ-InSe [37, 43–46], β-GaS [35, 42] and GaTe [42] at RT. The solid lines are plotted in accordance with equation (4). The experimental $\Phi_{bS}{}^{p}$ (Al, Cu, Pd) points for GaS represent the averaged values taken from [35, 42].

5. Metal/semiconductor interfaces

In the investigations of M/S structures the main attention is devoted to the barrier height Φ_{bS} dependence on the WF (Φ_m) of the contact metal. In the linear interface potential theory $\partial\Phi_{bS} = S{\cdot}\partial\Phi_m$, where the parameter S is constant for a given semiconductor. At the ideal M/S interface $S = 1$ (Schottky W 1940), while at the Fermi level pinning by the interface states $S = 0$ (Bardeen J 1947). Both models give the obscure results in most of cases and for the real M/S structures $0 < S < 1$. The barrier height at the M/S structures for electrons $\Phi_{bS}{}^{n}$ (holes $\Phi_{bS}{}^{p}$) in the general case can be estimated from the expressions [38]

$$\Phi_{bS}{}^{n} = \left(E_g\text{–CNL}\right) + S\left(\Phi_m\text{–CNL}^{abs}\right),$$
$$\Phi_{bS}{}^{p} = E_g\text{–}\Phi_{bS}{}^{n} = \text{CNL–}S\left(\Phi_m - \text{CNL}^{abs}\right), \qquad (4)$$

which at $S = 1$ correspond to the Schottky limit and at $S = 0$ —to the Bardeen limit. Here, the slope parameter $S = 1/[1+0.1(\varepsilon_\infty{}^{eff}-1)^2]$, where $\varepsilon_\infty{}^{eff} = (\varepsilon_{\infty\perp}\varepsilon_{\infty\parallel})^{1/2}$ [39]. In three-dimensional semiconductors the Fermi level at the M/S interface is pinned by the defect states while in two-dimensional III–VI semiconductors at (0001) van der Waals planes the defect states are absent as supposed and Fermi level is pinned by the metal induced tunnel gap states (TGS) mainly [40].

It is known that GaSe, InSe, GaS and GaTe semiconductors form rectifying barriers with a number of metals: (Cs, Li, Ca, Mg, Al, In, Sn, Ag, Cu, Au, Pd, Pt)/GaSe [41, 42], (Au, Ag, Al, Mg,)/GaTe [41], (Al, Au, ITO, Co, Pt, Sn, Sb, Zn)/InSe [37, 43–46], (Au, Ag, Al, Ga, Cu, Sn, Cu, Pd, Pb)/GaS [35, 42]. Some of these structures can be of technological interest, so we performed an analysis of the experimental barrier heights at M/S (ε-GaSe, γ-InSe, β-GaS and GaTe) versus Φ_m. We used the WFs of the contacting metals from [34] while for ITO we adopted WF = 4.3 eV [47].

To obtain values of S parameter for the compounds under study we employed the high-frequency dielectric constants $\varepsilon_{\infty\perp}$ and $\varepsilon_{\infty\parallel}$ available from the literature. Unfortunately, these data for some of III–VI materials are scanty and conflicting. For example, in case of GaS the following values of $\varepsilon_{\infty\perp}$ and $\varepsilon_{\infty\parallel}$ have been published: 5.0 and 3.8 (which results in the $S = 0.47$) [35], 6.7 and 5.3 ($S = 0.29$) [48], 6.31 and 4.95 ($S = 0.32$) [49] respectively. We used the following S values: GaSe ($S = 0.25$ [50]), InSe (0.21 [51]), GaTe ($S = 0.21$ [50]) and GaS (0.32 [49]).

The experimental $\Phi_{bS}{}^{p}$ data versus Φ_m for M/(ε-GaSe, γ-InSe, β-GaS and GaTe) together with the theoretical linear dependences calculated in accordance with equation (4) are presented in figure 2. As seen, the $\Phi_{bS}{}^{p}$ predictions from equation (4) are in close agreement with the experimental data in most cases. $\Phi_{bS}{}^{p}$ height is formed by the electrostatic dipole due to the difference between Φ_m and CNL^{abs} values and it is screened by the metal induced TGS. The zero net charge dipole at M/S interface takes place at $\Phi_m \approx \text{CNL}^{abs}$, that corresponds to $\Phi_{bS}{}^{p} \approx \text{CNL}$. At $\Phi_m > \text{CNL}^{abs}$ ($\Phi_{bS}{}^{p} < \text{CNL}$) and at $\Phi_m < \text{CNL}^{abs}$ ($\Phi_{bS}{}^{p} > \text{CNL}$) the positive and the negative charges respectively are present at the interface.

6. Semiconductor/semiconductor interfaces

Investigations of heterojunctions (HJs) based on (0001) III–VI semiconductors reveal that mechanical stresses in these structures are present only in the first atomic layers near the surface due to the weak interlayer coupling. This ability of stress relaxation is very useful for epitaxial growth of layers

with high crystalline perfection on the different substrates (a so-called van der Waals epitaxy), even in the case of a large lattice constants mismatch. In particular, a deposition of III–VI semiconductors onto Si [4, 32], GaAs [4] and even Al_2O_3 [5] substrates has been realized today. It was also proposed that III–VI ultrathin buffer layers introduced in the mismatched HJs such as GaAs/Si, ZnSe/Si, etc may improve the quality of the grown structures.

The band bending and discontinuity at the S/S interface are the main parameters which determine the performance of HJ devices. The conduction band offsets (CBO) and valence band offsets (VBO) are defined by the difference of the semiconductors WF and by the CNLs' energy positions at the semiconductors surfaces. In the three-dimensional semiconductors two types of the surface states at the interface are generated: first, the charged states formed by the broken bonds and second, the TGS formed by wave functions of both semiconductors. Since the (0001) plane of the III–VI compounds contains a hexagonally close-packed chalcogen layer without dangling bonds, the CNL position in this case depends only on the energy distribution of the TGS within the forbidden gap (the so-called intrinsic CNL, see table 2). In general case CBO at the HJ interface can be estimated using the equation [38]

$$\mathrm{CBO} = \left(E_g{}^{\mathrm{r}} - \mathrm{CNL}^{\mathrm{r}}\right) - \left(E_g{}^{\mathrm{l}} - \mathrm{CNL}^{\mathrm{l}}\right) - S\left(\mathrm{CNL_r}{}^{\mathrm{abs}} - \mathrm{CNL_l}{}^{\mathrm{abs}}\right). \quad (5)$$

Here, l and r denote the left and the right semiconductors forming the HJ, and S parameter is chosen for a wide-gap semiconductor. This equation at $S = 1$ expresses the well-known electron affinity rule (EAR, Anderson R L 1947) and at $S = 0$ the Fermi level pinning at the interface. In this paper we restrict our analysis by two HJs: (0001)InSe/(0001)GaSe and (0001)GaSe/(111)Si.

In spite of the large lattice mismatch (~7%) the good structural quality of InSe/GaSe HJs was found. It was estimated from the data of x-ray spectroscopy measurements that for such HJs the CBO is at about 0.7 eV and the VBO is at about or less than 0.1 eV [28]. The close VBO and CBO values at about 0.9 and 0.1 eV respectively were found from XPS measurements [52]. At the same time, application of the EAR model gives CBO = 0.84 eV and VBO = −0.09 eV, Fermi level pinning model gives CBO = 0.72 eV and VBO = 0.03 eV, while equation (5) produces CBO ≈ 0.75 eV and VBO ≈ 0.0 eV. As seen there is agreement between the CBO (VBO) for the InSe/GaSe HJ estimated from the various models. This agreement can be attributed to the close similarity of the corresponding $\mathrm{CNL}^{\mathrm{abs}}$ values for InSe and GaSe (table 2). In this case the net charge at the surfaces of semiconductors is close to zero and therefore all the models give practically the same results.

The structural and electronic properties of HJ (0001)GaSe/(111)Si (lattice mismatch ~2.45%) have been investigated in [4, 32]. For such HJ the authors of [32] from the photoemission spectroscopy measurements of WF(GaSe) = 4.6 ± 0.2 eV and EA(Si) = 4.0 eV estimated CBO = 0.2 ± 0.2 eV and VBO = 0.7 ± 0.2 eV using EAR. At the same time from the data of table 2 we obtain CBO = 0.27 eV and VBO = 0.63 eV taking into account the EAR. The Fermi level pinning model gives CBO = 0.46 eV and VBO = 0.43 eV, while equation (5) yields CBO = 0.50 eV and VBO = 0.40 eV. These results are believable and indicate that Fermi level at the (0001)GaSe/(111)Si interface is pinned near the CNL energies.

The performed estimations demonstrate that equation (5) gives realistic CBO and VBO values for HJs formed with III–VI semiconductors when using their intrinsic CNLs as input data.

7. Conclusions

The calculations of the band structure energies of ε-GaSe, γ-InSe, β-GaS and GaTe have been carried out by the DFT method using the optimized structural parameters obtained with van der Waals vdW-DF2-C09 density functional. The vdW-DF2-C09 functional, constructed with the inclusion of a specially designed non-local correlation term, is shown to outperform standard GGA functionals and for the III–VI compounds produces the values of interlayer distance and lattice constant c in close agreement with experiment.

The CNL energy position in ε-GaSe, γ-InSe, β-GaS and GaTe are calculated at temperatures close to 0 K and also at RT using the obtained band structures. These calculations reveal that CNL is located deeply in the lower half of the ε-GaSe, β-GaS and GaTe forbidden gaps and in the upper half of the forbidden gap in case of γ-InSe crystal. Thus, the predominantly p-type conductivity observed in the undoped GaSe, GaS and GaTe samples and n-type conductivity demonstrated by as-grown InSe can be explained by the specific position of CNL with respect to the edges of band gap.

The barrier heights at M/III–VI semiconductor interfaces and HJs based on the III–VI compounds have been estimated using the concept of the CNL. Reasonable agreement between the theoretical and experimental M/S barrier heights and the band offsets in the (0001)InSe/(0001)GaSe and (0001)GaSe/(111)Si HJs has been obtained.

Acknowledgments

This research was supported by Grants nos. 8.2.10.2015 and 8.2.06.2015 of Tomsk State University Academic D I Mendeleev Fund Program.

References

[1] Gouskov A, Gamassel J and Gouskov L 1982 Growth and characterization of III-V layered crystals like GaSe, GaTe, InSe, $GaSe_{1-x}Te_x$ and $Ga_xIn_{1-x}Se$ *Prog. Cryst. Growth Charact.* **5** 323–413

[2] Gomes da Costa P, Dandrea R G, Wallis R F and Balkanski M 1993 First-principles study of the electronic structure of γ-InSe and β-InSe *Phys. Rev.* B **48** 14135–41

[3] Sanchez-Royo J F, Segura A, Lang O, Schaar E, Pettenkofer C, Jaegermann W, Roa L and Chevy A 2001 Optical and photovoltaic properties of indium selenide thin films prepared by van der Waals epitaxy *J. Appl. Phys.* **90** 2818–23

[4] Amimer K, Eddrief M and Sebenne C A 2000 Stress relaxation at forming GaSe-Si(111) interfaces *J. Cryst. Growth* **217** 371–7

[5] Chegwidden S and Dai Z 1998 Molecular beam epitaxy and interface reactions of layered GaSe growth on sapphire (0001) *J. Vac. Sci. Technol.* A **16** 2376–80

[6] Rak Z, Mahanti S D, Mandal K C and Fernelius N C 2009 Theoretical studies of defect states in GaTe *J. Phys.: Condens. Matter.* **21** 015504

[7] Ghalouci L, Benbahi B, Hiadsi S, Abidri B, Vergoten G and Ghalouci F 2013 First principle investigation into hexagonal and cubic structures of Gallium Selenide *Comput. Mater. Sci.* **67** 73–82

[8] Olguin D, Rubio-Ponce A and Cantarero A 2013 *Ab initio* electronic band structure study of III–VI layered semiconductors *Eur. Phys. J.* B **86** 350

[9] Lee K, Murray E D, Kong L, Lundqvist B I and Langreth D C 2010 Higher-accuracy van der Waals density functional *Phys. Rev.* B **82** 081101(R)

[10] Cooper V R 2010 Van der Waals density functional: An appropriate exchange functional *Phys. Rev.* B **81** 161104(R)

[11] Grimme S 2006 Semiempirical GGA-type density functional constructed with a long-range dispersion correction *J. Comput. Chem.* **27** 1787–99

[12] Brudnyi V N, Kosobutsky A V and Sarkisov Yu S 2010 Charge neutrality level and electronic properties of GaSe under pressure *Semiconductors* **44** 1158–66

[13] Kosobutsky A V, Sarkisov S Y and Brudnyi V N 2013 Structural, elastic and electronic properties of GaSe under biaxial and uniaxial compressive stress *J. Phys. Chem. Solids* **74** 1240–8

[14] Giannozzi P *et al* 2009 QUANTUM ESPRESSO: a modular and open-source software project for quantum simulations of materials *J. Phys.: Condens. Matter.* **21** 395502

[15] Perdew J P, Burke K and Ernzerhof M 1996 Generalized gradient approximation made simple *Phys. Rev. Lett.* **77** 3865–8

[16] Kuhn A, Chevy A and Chevalier R 1976 Refinement of the 2H GaS p-type *Acta Cryst.* **B32** 983–4

[17] Cenzual K, Louise L, Gelato M, Penzo M and Parthe E 1991 Inorganic structure types with revised space groups *Acta Cryst.* **B47** 433–9

[18] Rigoult J, Rimsky A and Kuhn A 1980 Refinement of the 3R γ-indium monoselenide structure type *Acta Cryst.* **B36** 916–8

[19] Julien-Pouzol P M, Jaulmes S, Guittard M and Alapini F 1979 Monotellurure de gallium, GaTe *Acta Cryst.* **B35** 2848–51

[20] Kosobutsky A V and Basalaev Y M 2010 First principles study of electronic structure and optical properties of $LiMTe_2$ (M = Al, Ga, In) crystals *J. Phys. Chem. Solids* **71** 854–61

[21] Kosobutsky A V and Basalaev Y M 2014 Electronic band structure of $LiInSe_2$: a first-principles study using the Tran-Blaha density functional and GW approximation *Solid State Commun.* **199** 17–21

[22] Aulich E, Brebner J L and Mooser E 1969 Indirect energy gap in GaSe and GaS *Phys. Status Solidi* B **31** 129–31

[23] Camassel J, Merle P, Mathieu H and Chevy A 1978 Excitonic absorption edge of indium selenide *Phys. Rev.* B **17** 4718–25

[24] Camassel J, Merle P, Mathieu H and Gouskov A 1979 Near-edge-band optical properties of $GaSe_{(x)}Te_{(1-x)}$ mixed crystals *Phys. Rev.* B **19** 1060–8

[25] Ho C H and Lin S L 2006 Optical properties of the interband transitions of layered gallium sulfide *J. Appl. Phys.* **100** 083508

[26] Brudnyi V N, Grinyaev S N and Stepanov V E 1995 Local neutrality conception: Fermi level pinning in defective semiconductors *Physica* B **212** 429–35

[27] Brudnyi V N, Grinyaev S N and Kolin N G 2004 A model for Fermi-level pinning in semiconductors: radiation defects, interface boundaries *Physica* B **348** 213–25

[28] Tasuyama C, Tanbo T and Nakayama N 1990 Heteroepitaxy between layered semiconductors GaSe and InSe *Appl. Surf. Sci.* **41-2** 539–43

[29] Williams R H, McGovern I T, Murray R B and Howells M 1976 An investigation of the electronic structure of GaSe and GaTe by photoelectron spectroscopy, using a synchrotron source, and electron energy loss spectroscopy *Phys. Status Solidi* B **73** 307–16

[30] Williams R H and McEvooy A J 1972 Surface properties of the gallium monochalcogenides *Phys. Status Solidi* A **12** 277–86

[31] Gobelly G W and Allen F G 1965 Photoelectric properties of cleaved GaAs, GaSb, InAs and InSb surfaces: comparison with Si and Ge *Phys. Rev.* A **137** 245–54

[32] Reqqass H, Lacharme J-P, Sebenne C A, Eddrief M and Thanh V Le 1996 Surface electronic properties of GaSe-covered Si(111) upon UHV thermal desorption of the GaSe epitaxial layer *Appl. Surf. Sci.* **92** 357–61

[33] Williams R H and McEvooy A J 1972 Electron emission studies from GaSe surface *J. Vac. Sci. Technol.* **9** 867–70

[34] Lide D R (ed) 2004 *CRC Handbook of Chemistry and Physics* 85th edn (Boca Raton, FL: CRC Press) p 2712

[35] van den Dries J G A M 1976 Schottky barrier on the layer compound gallium sulfide *PhD Thesis* Eindhoven p 87

[36] Mandal K C, Hayhes T, Muzykov P G, Krishna R, Das S, Sudarshan T S and Ma S 2010 Characterization of Gallium Telluride crystals grown from graphite crucible *Proc. SPIE* **7805** 78050Q-1-10

[37] Martinez-Pastor J, Segura A and Valdes J L 1987 Electrical and photovoltaic properties of indium-tin-oxide/p-InSe/Au solar cells *J. Appl. Phys.* **62** 1477–83

[38] Robertson J and Falabretti B 2006 Band offsets of high K gate oxides on III–V semiconductors *J. Appl. Phys.* **100** 014111

[39] Monch M 1987 Role of virtual gap states and defects in metal-semiconductor contacts *Phys. Rev. Lett.* **58** 1260–3

[40] Tersoff J 1984 Schottky barrier heights and the continuum of gap states *Phys. Rev. Lett.* **52** 465–8

[41] Kurtin S, McGill T S and Mead C A 1971 Direct interelectrode tunneling in GaSe *Phys. Rev.* B **3** 3368–79

[42] Kurtin S and Mead C A 1969 Surface barriers on layer semiconductors: GaS, GaSe, GaTe *J. Chem. Sol.* **30** 2007–9

[43] Hasegawa I and Abe Y 1982 Electrical and optical characteristics of a Schottky barrier on a cleaved surface of the layered semiconductor InSe *Phys. Status Solidi* A **70** 615–21

[44] Di Giulio M, Micocci G, Rizzo A and Tepore A 1983 Photovoltaic effect in gold-indium selenide Schottky barriers *J. Appl. Phys.* **54** 5839–43

[45] Mamy R, Zaoui X, Barrau J and Chevy A 1990 Au/InSe Schottky barrier height determination *Rev. Phys. Appl.* **25** 947–50

[46] Duman S, Elkoca Z, Gurbulak B, Bahntiyari T T and Dogan C 2012 Metal/p-InSe:Mn Schottky Barriers Diodes *J. Optoelectron. Adv. Mater.* **14** 693–8

[47] Sugiyama K, Ishii H, Ouchi Y and Seki K 2000 Dependence of indium-tin-oxide work function on surface cleaning method as studied by ultraviolet and x-ray photoemission spectroscopies *J. Appl. Phys.* **87** 295–8

[48] Riede V, Neumann H, Hoang X N, Sobotta H and Levy F 1980 Polarization-dependent infrared optical properties of GaS *Physica* B + C **100** 355–63

[49] Segura A and Chevy A 1994 Large increase of the low-frequency dielectric constant of gallium sulfide under hydrostatic pressure *Phys. Rev.* B **49** 4601–4

[50] Leung P C, Andermana G, Spitzer W G and Mead C A 1966 Dielectric constants and infrared absorption of GaSe *J. Phys. Chem. Sol.* **27** 849–55

[51] Adachi S 2012 *The Handbook on Optical Constants of Semiconductors: In Tables and Figures* (Singapore: World Scientific) p 632

[52] Lang O, Klein A, Jaegermann W and Chevy A 1996 Band lineup of lattice mismatched InSe/GaSe quantum well structures prepared by van der Waals epitaxy: absence of interfacial dipoles *J. Appl. Phys.* **80** 3817–21